

Chapter 8

Investigating Charge Transport Through RPA-Bound Single-Stranded DNA Using Covalent Photooxidants

This work was part of a collaboration with A. Ehlinger and W. Chazin at Vanderbilt University.

P. Bartels performed all DNA preparation and purification, and carried out all photooxidation experiments and associated analysis. A. Ehlinger expressed and purified RPA.

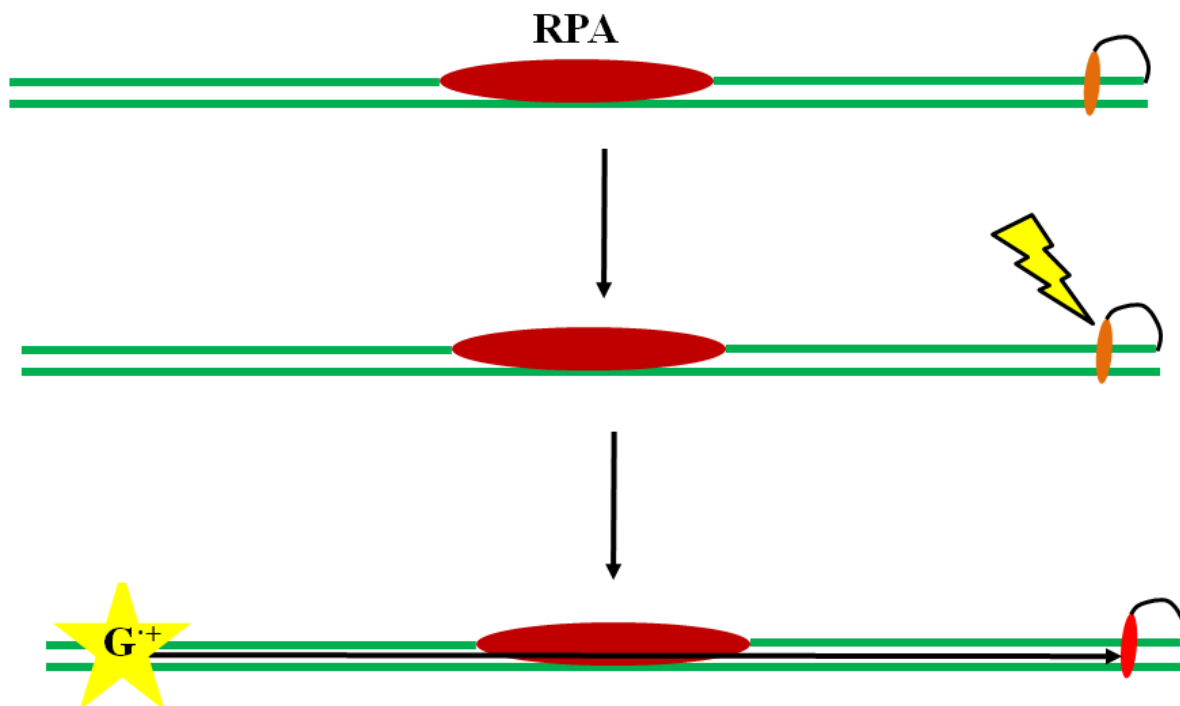
Introduction

Eukaryotic DNA replication involves a host of proteins that must coordinate their activity, both to accomplish their task in general and to respond to DNA damage and other setbacks collectively referred to as replication stress (*1, 2*). Of interest with respect to the stress response, several eukaryotic DNA replication and repair proteins, specifically DNA primase, DNA polymerase (Pol) δ , and MUTYH, have been shown to contain redox-active [4Fe4S] clusters (*3-5*). While redox-activity has not yet been demonstrated, [4Fe4S] clusters are also present in Pol ϵ , the helicase-nuclease Dna2, the translesion synthesis polymerase Pol ζ , and the endonuclease III homologues Ntg2/NTHL1 (yeast and human names, respectively) (*6-10*). Among those proteins previously studied, all were shown to be capable of long-range DNA-mediated charge transport (DNA CT) (*3, 4*). DNA CT, in which electrons and holes travel rapidly over long molecular distances through the π -stacked DNA base pairs, exhibits an acute sensitivity to even slight perturbations in base pair stacking and is thus an excellent reporter of damage (*11*). Indeed, electrochemical studies have shown dramatic CT attenuation by a wide variety of different lesions (*12*). DNA CT, however, is a phenomenon exclusive to duplexed DNA, while DNA replication involves a significant amount of single-stranded DNA, limiting the range of communication between redox-active proteins in this context.

At the replication fork, unwound single stranded DNA is coated with the single-stranded binding protein replication protein A (RPA) (*1*). RPA is a heterotrimeric complex consisting of three subunits: RPA70, RPA32, and RPA14 (*13*). Among these subunits are four DNA binding domains, which act sequentially in three binding modes to enhance binding affinity. These are an 8-10 nucleotide (nt) mode, a 25 nt mode, and an intermediate 12-22 nt binding mode (*13*). Crystal structures of the DNA binding domains show stacking interactions between aromatic

residues in RPA and the bases of single-stranded DNA, raising the intriguing possibility of CT through RPA-coated DNA during replication (14). Indeed, aromatic residues have been shown to couple with duplexed DNA in HhaI, ensuring that such a prospect is feasible (15). Notably, a structure of the entire complex bound to DNA shows a U-shaped bend that may be problematic for CT (16). However, the bend is not sharp, and CT can certainly occur through wrapped DNA as long as local base stacking remains intact (17). Furthermore, crystal structures show only a single conformation, and the situation in solution is likely to be far more dynamic. In any case, even if CT were not possible in this binding mode, the shorter modes remain of interest. If it can occur, CT through RPA-bound DNA would dramatically expand the possible communication pathways in DNA replication, and is thus worth investigating.

To test the possibility of CT through RPA-bound DNA, we have designed a system consisting of a DNA duplex with a covalent photooxidant on one end and containing an RPA-sized gap in the middle (Scheme 8.1). Taking advantage of the propensity of damage to localize on guanine multiplets (guanine has the highest oxidation potential of the DNA bases) (18), we aimed to evaluate damage on DNA irradiated in the presence and absence of RPA. These experiments are ongoing and represent a first step toward addressing the possibility of CT through single-stranded DNA at the replication fork, and future efforts should shed light on this intriguing possibility.



Scheme 8.1 Photooxidation scheme to test CT through RPA-coated ssDNA. In these experiments, RPA binds a single-stranded gap in a DNA substrate containing a photooxidant (orange) at one end. Irradiation will excite the photooxidant and provide a driving force for guanine oxidation. If CT can occur through RPA-bound DNA, guanine radical will form on the other end of the gap, resulting in damage products that can be cleaved by piperidine. Appending a 5' ³²P label to this strand will allow cleavage products to be visualized.

Materials and Methods

Protein Expression and Purification

Heterotrimeric yeast RPA was overexpressed and purified as previously described (19).

DNA Synthesis and Purification

Unmodified DNA oligomers were purchased from IDT and purified by HPLC. DNA for conjugation to anthraquinone (AQ) or rhodium photooxidants was prepared on an Applied Biosystems automated DNA synthesizer. For AQ conjugation, 3' C3 amino-modified CPG beads were purchased from Glen Research (3'-PT-Amino-Modifier C3 CPG). After synthesis, DNA was deprotected with 28-30% ammonium hydroxide (Sigma-Aldrich) (8 hrs, 65 °C), filtered, and purified by HPLC (Agilent PLRPS column, 5-75% ACN/95-25% 50 mM ammonium acetate gradient over 30 minutes at a flow rate of 2 mL/min). The terminal DMT group was removed by 30' RT incubation in 80% aqueous acetic acid, and the DNA was HPLC purified a second time (PLRPS column, 5-15% ACN/95-85% 50 mM ammonium acetate over 35 minutes at a 2 mL/min flow rate). DNA was then desalted by standard EtOH precipitation.

5' ³²P labeling was achieved by incubating 50 pmol freshly prepared single-stranded DNA with T4 polynucleotide kinase (PNK; New England Biolabs) and [γ -³²P] ATP (Perkin Elmer) for 30 minutes at 37 °C. PNK was heat inactivated (10 minutes, 85 °C) and DNA was isolated from unreacted radiolabeled ATP by running samples through MicroBioSpin6 columns (BioRad) according to product instructions.

Once all DNA oligomers were prepared, the appropriate strands were quantified by UV-visible spectroscopy using molar extinction coefficients from IDT and annealed in equimolar ratios (5 minutes at 95 °C followed by cooling to RT over 1.5-2 hours) in storage buffer (5 mM sodium phosphate, pH 7.0, 50 mM NaCl). DNA substrate design consisted of 1 long strand

annealed to two complements with an RPA-appropriate gap in between. The DNA strand on one side of the gap contained a 5' ³²P label and a guanine doublet to serve as a hole trap, while the strand on the other side contained either an AQ or rhodium photooxidant covalently tethered to the 5' end. For comparison with RPA-bound DNA, a DNA sequence complementary to the gap was included as a control. The DNA sequences for photooxidation experiments were as follows:

AQ DNA

³²P 29-mer: ³²P - 5' - TGT ACG ACA GGT GTC ATG CTA GCA TCA TA - 3'

16-mer AQ: 5' - ACA CTA TAG CTC AGA G - 3' - AQ

55-mer: 5' - CTC TGA GCT ATA GTG TGA CGT TCG AGA TCA CGT CAT ATG ATG CTA GCA T - 3'

15-mer: 5' - GAC ACC TGT CGT ACA - 3'

40-mer: 5' - CTC TGA GCT ATA GTG TAC GTC GCA CAT ATG ATG CTA GCA T - 3'

10-mer gap: 5' - TGT GCG ACG T - 3'

25-mer gap: 5' - TGA CGT CAA CGT GAT CTC GAA CGT C - 3'

Rh DNA

Rh 16-mer: Rh - 5' - ACA CTA TAG CTC AGA C - 3'

³²P 15-mer: ³²P - 5' - TGT AGG ATG CAG TCG - 3'

56-mer: 5' - CGA CTG CAT CCT ACA ACT GCA GTT GCA CTA GAG CTT GCA GCT CTG AGC TAT AGT GT - 3'

25-mer gap: 5' - CTG CAA GCT CTA GTG CAA CTG CAG T - 3'

Coupling Anthraquinone 2-Carboxylic Acid (AQ) to DNA

To couple AQ to DNA, anthraquinone 2-carboxylic acid (Sigma-Aldrich, 0.022 mmol) was activated to the NHS ester by dissolving in DMF (~500 μL) and stirring overnight in the

presence of *N,N'*-Dicyclohexylcarbodiimide (DCC; Sigma-Aldrich, 0.045 mmol) and *N*-hydroxysuccinimide (NHS; Sigma-Aldrich, 0.045 mmol). The reaction was then dried and the components redissolved in a minimal amount of DMSO (~600 μ L). Dried amino-modified DNA was dissolved in 200 μ L 100 mM sodium bicarbonate and 50 μ L of activated AQ NHS ester was added to each tube and gently shaken in the dark overnight. DNA was isolated by NAP-5 column (GE Healthcare) and HPLC purified a final time using the same method as the second purification. MALDI-TOF mass spectrometry was used to confirm the mass of the oligomer.

Coupling [Rh(phi)₂bpy']³⁺ to DNA

For rhodium conjugation, DNA was prepared on the synthesizer using CPG beads with 2000 Å pore size (20). The terminal DMT group was cleaved on the column as the final step of the synthesis to expose the 3' hydroxyl group for further reactions. Once synthesized, the CPG beads were added directly to a 2.5 cm x 10 cm glass cylinder with a glass frit and stopcock. The cylinder was sealed from above and connected to an aspirator, and the beads were washed 3x with 3 mL dry 1,4 dioxane (Sigma-Aldrich). 0.308 mmol (50 mg) carbonyldiimidazole (CDI; Sigma-Aldrich) was dissolved in dry dioxane and added directly to the beads; this mixture was gently shaken for 30 minutes. The beads were then dried and washed 5x with 3 mL dry dioxane, and a 1 mL solution of 1,9 diaminononane (0.202 mmol; 32 mg) in 9:1 dioxane:water was added and the reaction gently stirred at RT for 25 minutes (Scheme 8.2). Following reaction, the beads were rinsed 3x each in dry dioxane followed by MeOH.

[Rh(phi)₂bpy']Cl₃ was prepared as previously described (21), and the structure confirmed with ¹H NMR in deuterated water (Figure 8.2). To prepare for 5' coupling, [Rh(phi)₂bpy']Cl₃ (0.013 mmol; 11.4 mg) was placed in a scintillation vial and dissolved in a minimal volume of 1:1:1 dry CH₃OH/CH₂Cl₂/CH₃CN along with 0.027 mmol (8.1 mg) *N,N,N',N'*-Tetramethyl-O-

(N-succinimidyl)uronium tetrafluoroborate (TSTU). The reaction was started by adding 0.034 mmol (5.92 μ L) N,N-Diisopropylethylamine (DIEA) and stirred at RT for one hour (Scheme 8.3). Immediately after addition of DIEA, the solution went from orange to dark red. After one hour, a small sample was analyzed by ESI mass spectrometry, which yielded two major peaks at 866 Da and 994 Da (Figure 8.3). The peak at 866 Da consistent with NHS ester formation accompanied by loss of two protons from the phi ligand imine nitrogen atoms in DIEA, while that at 994 Da is attributable to TSTU coupled directly to the bpy' carboxylic acid through the imine group.

After TSTU activation, the DNA beads were added directly to the rhodium reaction mix and stirred overnight (Scheme 8.4). Alternatively, the rhodium solution was added to the beads on the glass cylinder and shaken overnight; both methods produced equivalent yields. In both cases, the beads were placed on the glass cylinder, dried, and washed successively (3x each) with dry MeOH, CH₂Cl₂, and ACN. Even after drying, the beads remained orange, confirming successful coupling (Figure 8.4). Notably, the beads are strongly solvatochromic, appearing palest in MeOH and darkest in CH₂Cl₂, with intermediate intensity in ACN (Figure 8.4). Once rinsed, DNA was removed from the beads by incubation with 800 μ L 28-30% ammonium hydroxide (Sigma-Aldrich) for 6 hours at 60 °C.

Isolated DNA was dried on a speed vacuum, dissolved in 600 μ L buffer (5 mM sodium phosphate, pH 7.0, 50 mM NaCl), filtered, and purified by HPLC (PLRPS column, 5-15% ACN/95-85% 50 mM ammonium acetate gradient over 35 minutes, 2 mL/min flow rate). To ensure collection of coupled DNA, absorbance was monitored at 260, 280, and 360 nm; two major peaks (consistent with previous reports and corresponding to separate enantiomers) eluted around 22 and 28 minutes (Figure 8.5). MALDI-TOF mass spectrometry was used to confirm the

identity of the DNA; a mass of 5819 Da was obtained, very close to the expected mass of 5814 Da. DNA was quantified by UV-visible spectroscopy using a molar extinction coefficient at 390 nm of $19000 \text{ M}^{-1}\text{cm}^{-1}$ for Rh-tethered DNA (Figure 8.6) (20).

Photooxidation Reactions with RPA

Reaction mixes (30 – 50 μL) consisted of 133 nM DNA (2 pmol) with a 0, 1, 5, or 10-fold molar excess of RPA, 0.2 mg/mL BSA, 150 mM NaCl, 50 mM Tris-HCl, pH 7.8, and 10% glycerol v/v. Samples were prepared in Eppendorf tubes, incubated at 37 °C for one minute to facilitate RPA binding, and transferred to glass vials for photooxidation. Photooxidation was accomplished by irradiation (30 minutes or 1 hour) under a solar simulator with a UVB/C filter applied, after which reactions were transferred back into Eppendorf tubes and dried on a speed vacuum. To cleave the DNA at sites of damage, dried DNA was dissolved in 100 μL buffer (50 mM Tris-HCl, pH 7.8, 150 mM NaCl) containing 10% piperidine by volume. This solution was then incubated 30 minutes at 90 °C, then precipitated in 1 mL chilled EtOH, left on dry ice 30 minutes, and spun down at 14000x g. The supernatant was removed, taking care to ensure that the bulk of the radioactivity remained in the tube, and samples were dried on the speed vacuum. Samples were then washed 3x in water and counted on a liquid scintillation counter prior to drying a final time. Dried samples were dissolved in 2 μL formamide loading dye, heated to 90 °C for 5 minutes, and equivalent amounts of radioactivity were loaded directly onto a 20% denaturing polyacrylamide gel. Electrophoresis was carried out at 90 W power for ~2 hours, or until the dye had migrated ~3/4 the length of the gel. Gels were then exposed (1 hour for every 300000 cpm) and imaged on a Typhoon phosphorimager; bands were quantified using ImageQuant software.

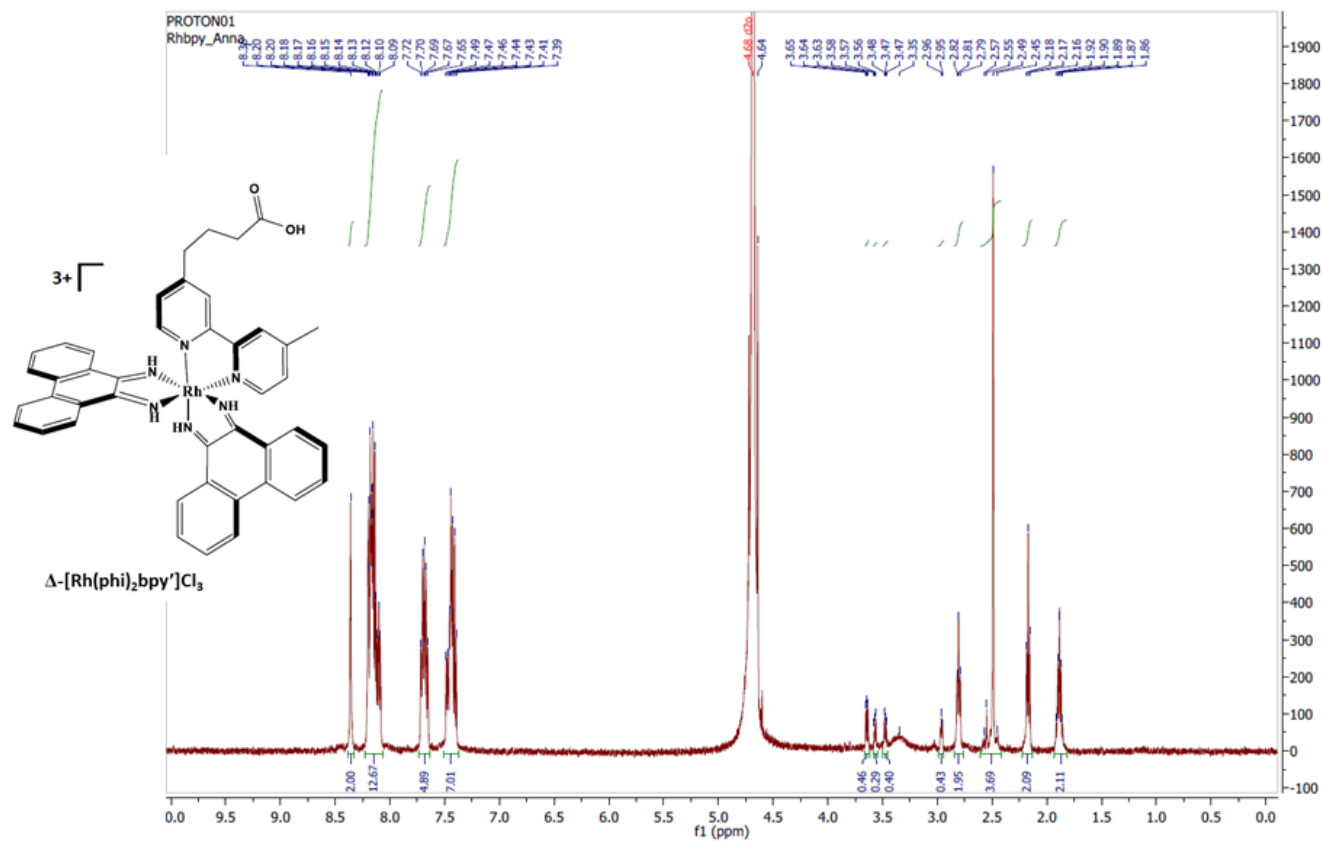
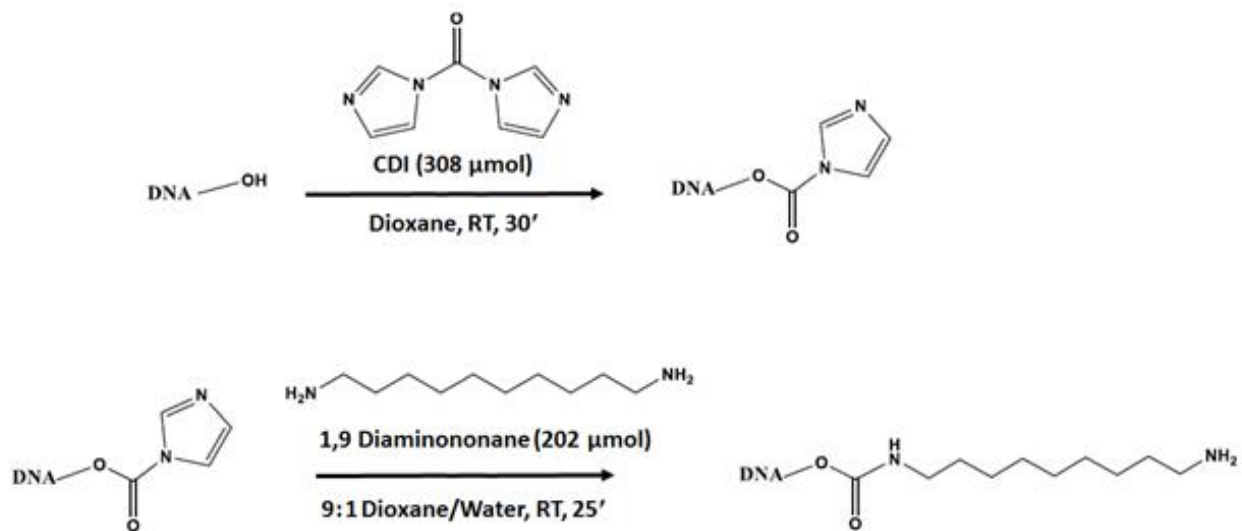
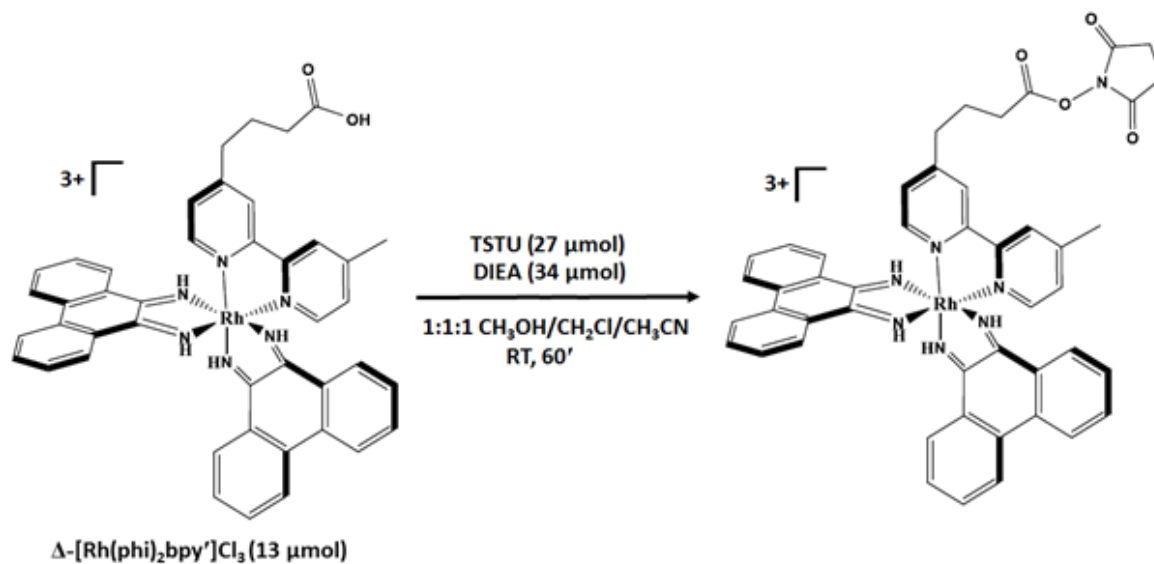


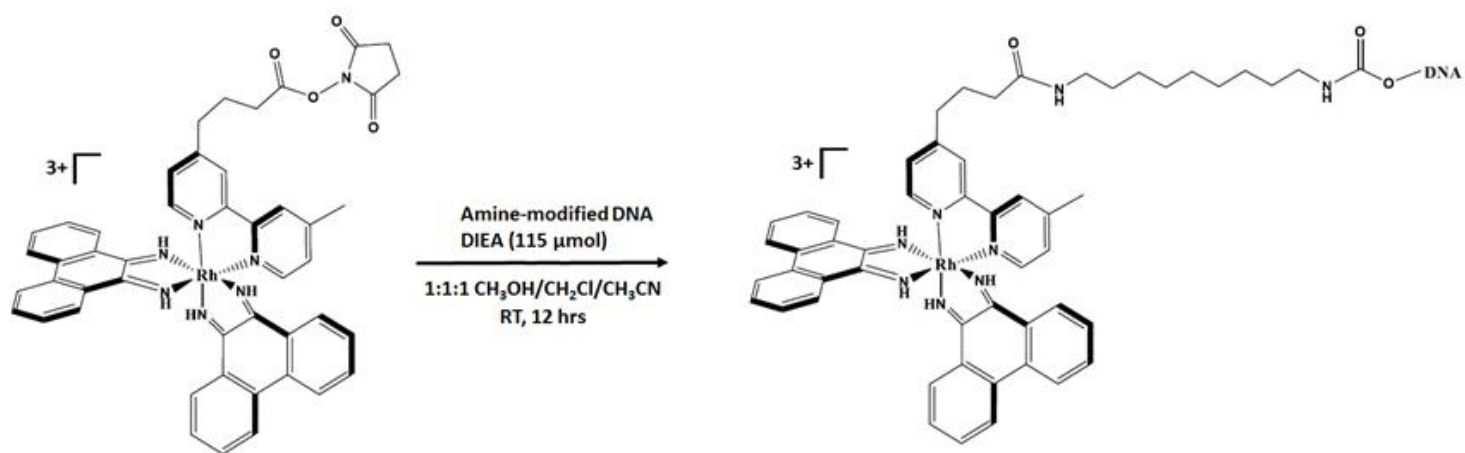
Figure 8.2 ^1H NMR spectrum of $[\text{Rh}(\text{phi})_2\text{bpy}]^{3+}$. All peaks integrate to the expected proportions, and are in agreement with previous studies (20).



Scheme 8.2 Amino modification of DNA on CPG beads with the DMT group removed.



Scheme 8.3 TSTU activation of [Rh(phi)₂bpy']³⁺ for coupling to amino-modified DNA. NHS ester formation is shown, but ESI-MS (Figure 8.3) confirms that this is one of two products along with a direct conjugation of TSTU at the imine group.



Scheme 8.4 Coupling of amino-modified DNA to activated $[\text{Rh}(\text{phi})_2\text{bpy}']^{3+}$.

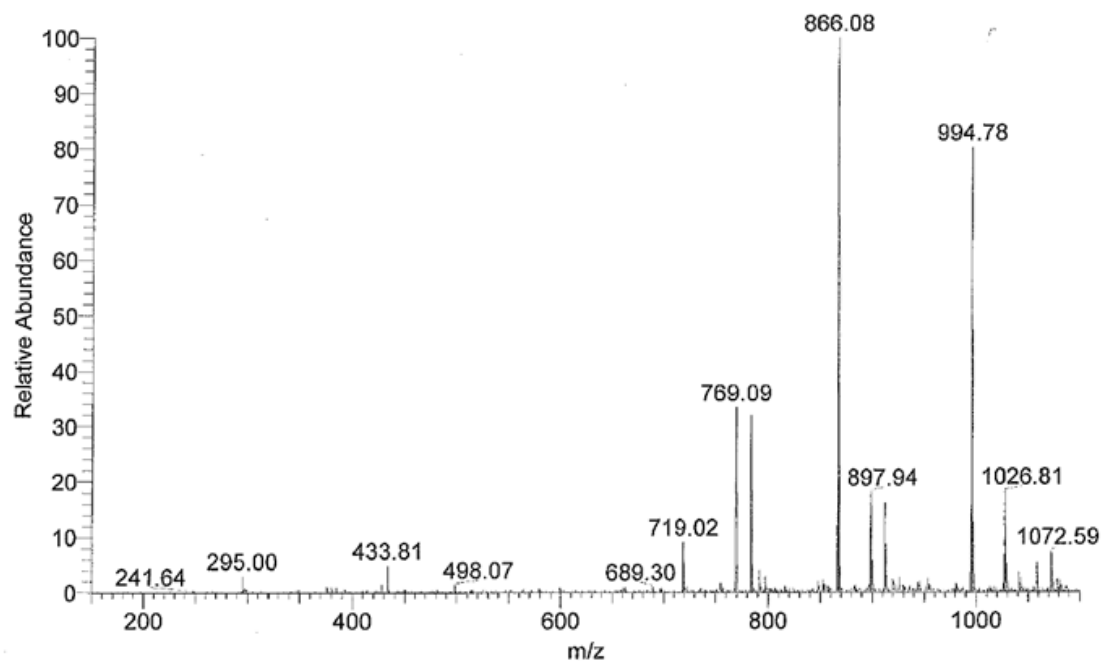


Figure 8.3 ESI-MS spectrum of $[\text{Rh}(\text{phi})_2\text{bpy}]^+$ after 1 hour of TSTU activation in 1:1:1 $\text{CH}_3\text{OH}/\text{CH}_2\text{Cl}_2/\text{CH}_3\text{CN}$ with DIEA present. The major peaks at 866 Da and 994 Da are consistent with NHS ester formation and direct $[\text{Rh}(\text{phi})_2\text{bpy}]$ TSTU coupling, respectively.

After Overnight Reaction



MeOH



CH₂Cl₂



CH₃CN



Figure 8.4 DNA on CPG beads post-Rh coupling and in a series of solvent washes.

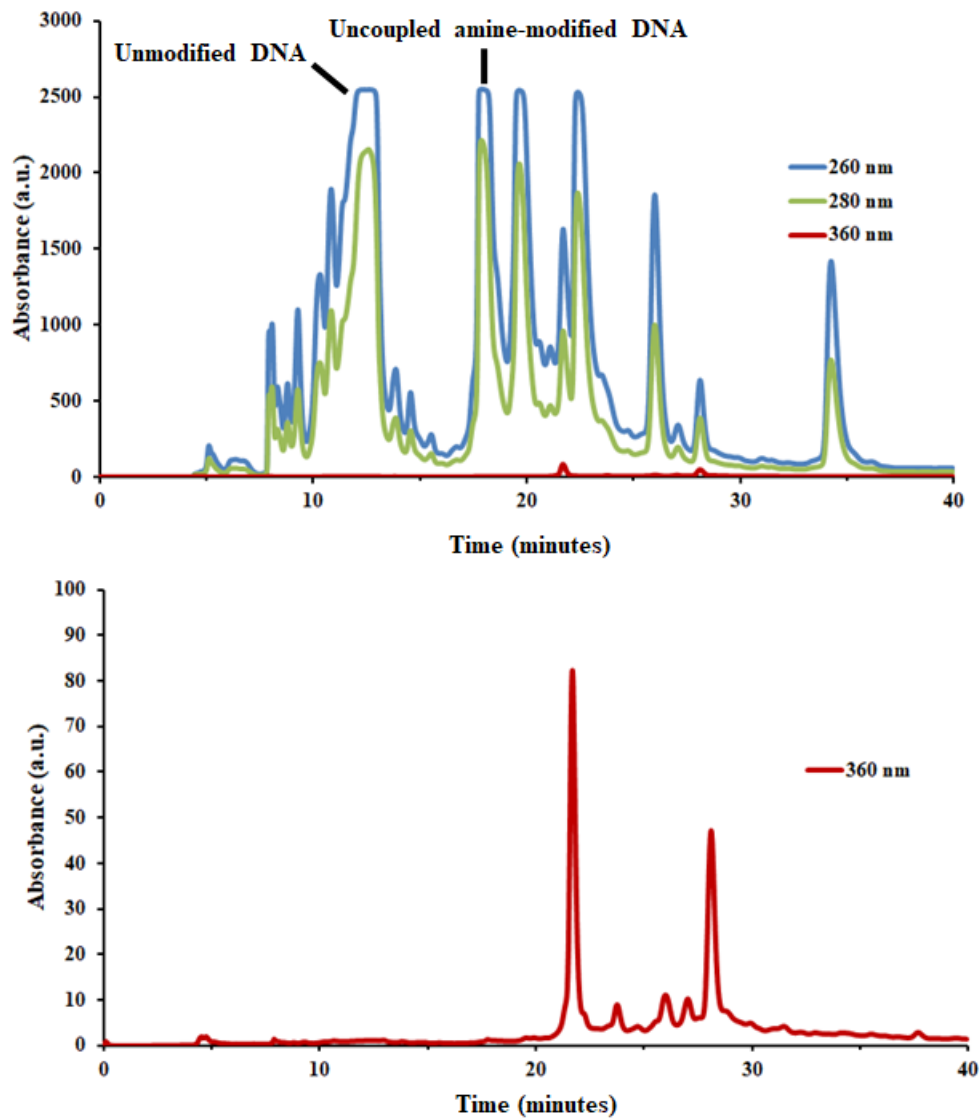


Figure 8.5 HPLC traces for Rh-conjugated DNA with UV-visible absorbance monitored at 260 and 280 nm to track DNA and 360 nm to track Rh. Peaks eluted around 12 minutes (unmodified DNA), 18-22 minutes (amino-modified DNA), and 21 and 28 minutes (Rh-coupled DNA).

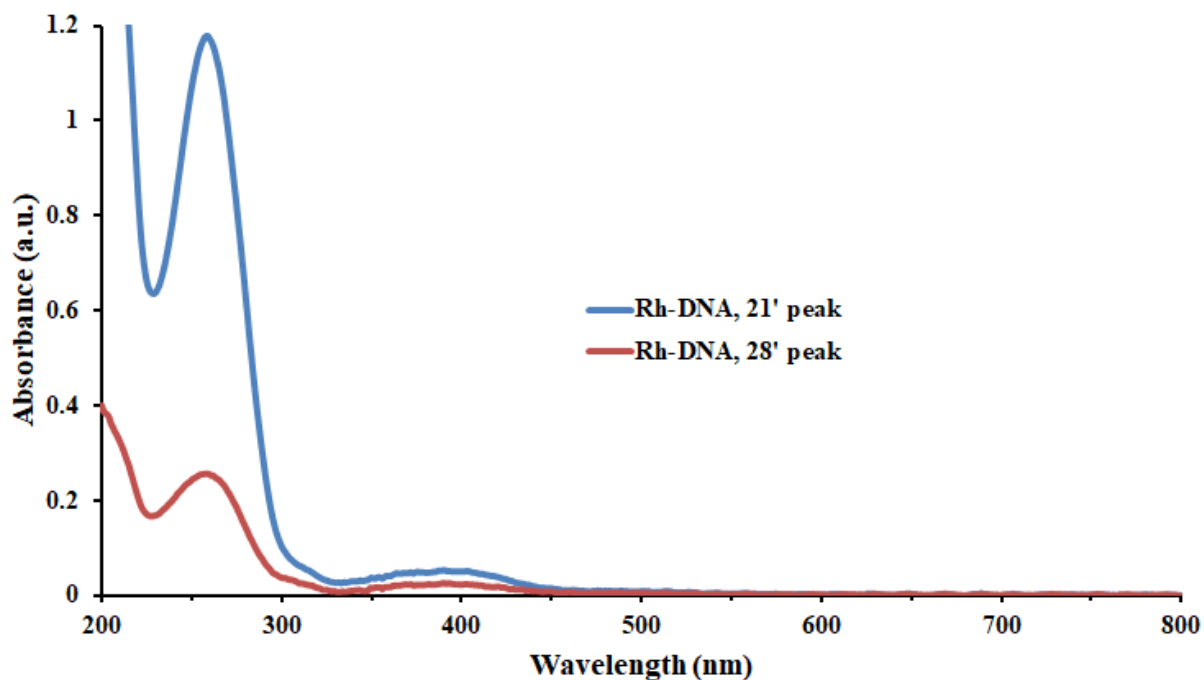


Figure 8.6 UV-visible spectra of 16-mer Rh-modified DNA. The UV-visible spectrum contains the broad peak centered at 390 nm expected for DNA-bound $[\text{Rh}(\text{phi})_2\text{bpy}]^{3+}$ conjugated to DNA. The two peaks shown are from different collections from HPLC representing different enantiomers.

Results and Discussion

RPA Reactions with Photooxidation by AQ

In AQ reactions, DNA was incubated with increasing concentrations of RPA, and control reactions lacking RPA and containing a fully duplexed substrate were subjected to the same treatment as RPA reactions. DNA containing both a 10-mer and a 25-mer gap was used to assess CT in RPA bound in its shortest and longest binding modes, respectively. From the polyacrylamide gels (Figure 8.7), it is apparent that the majority of DNA substrate (78% or more by band volume) did not cleave in any reaction. However, the reactions with 25 nM RPA on a 10-mer gapped substrate and 10 nM RPA on a 25-mer gapped substrate do show some low molecular weight bands representing 2-5% of the total radioactivity present. Using Maxam-Gilbert sequencing lanes as a guide, DNA cleavage, when present, occurred primarily at the expected GG site, but products are also present at the neighboring G and A positions. Overall, these results provide an intriguing start, but low photooxidation yields make it impossible to say if RPA had any effect, as even what little DNA damage is present does not occur with any particular pattern on either the 10- or 25-mer gapped substrates.

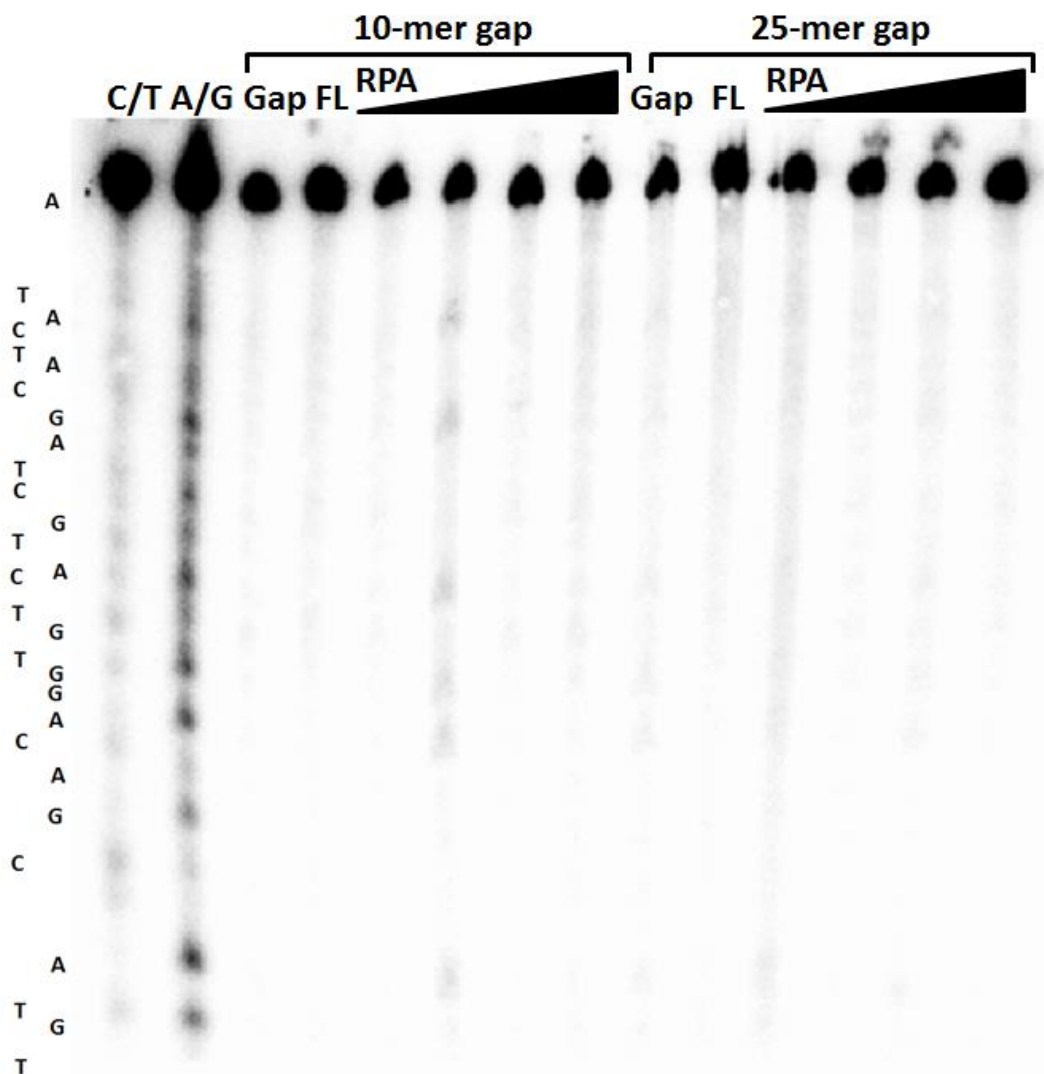


Figure 8.7 RPA reactions visualized on a 20% denaturing polyacrylamide gel. Based on Maxam-Gilbert sequencing lanes, several RPA reactions (25 nM RPA on 10-mer gap DNA and 10 nM RPA on 25-mer gap DNA) show damage at A/G sites representing 2-5% of the sample, but low yields prevent further analysis.

RPA Reactions with a Rh-Based Photooxidant

To improve oxidation yields, the photooxidant in our system was switched to $[\text{Rh}(\text{phi})_2\text{bpy}]^{3+}$. $[\text{Rh}(\text{phi})_2\text{bpy}]^{3+}$ yields are reported to be higher when covalently tethered to the 5' end of single stranded DNA, so the polarity of the modifier was reversed. To simplify substrate preparation, however, the 15-mer sequence used in AQ DNA was eliminated and the sequences were adjusted to leave only three components for RPA reactions (four for fully duplexed controls). Finally, to facilitate troubleshooting, only the 25-mer gapped substrate was investigated in these experiments, and irradiation time was increased to one hour in an effort to further enhance yields.

At this point, data from gels are inconclusive for several reasons (Figure 8.8). In all experiments, indiscriminate DNA cleavage was observed. In early experiments, this was likely due to excessive cutting by piperidine in water rather than buffer. Extra care was taken in later efforts to treat with piperidine in buffer and to remove it through extensive washing and drying steps. Unfortunately, the result of this prolonged treatment (1 week in total) was likely ^{32}P -induced damage; supporting this, Maxam-Gilbert sequencing lanes prepared at the same time and treated in the same way also show indiscriminate cleavage. In summary, the problems encountered in these early efforts are expected to be simple to overcome, and future experiments will likely yield more fruitful results.

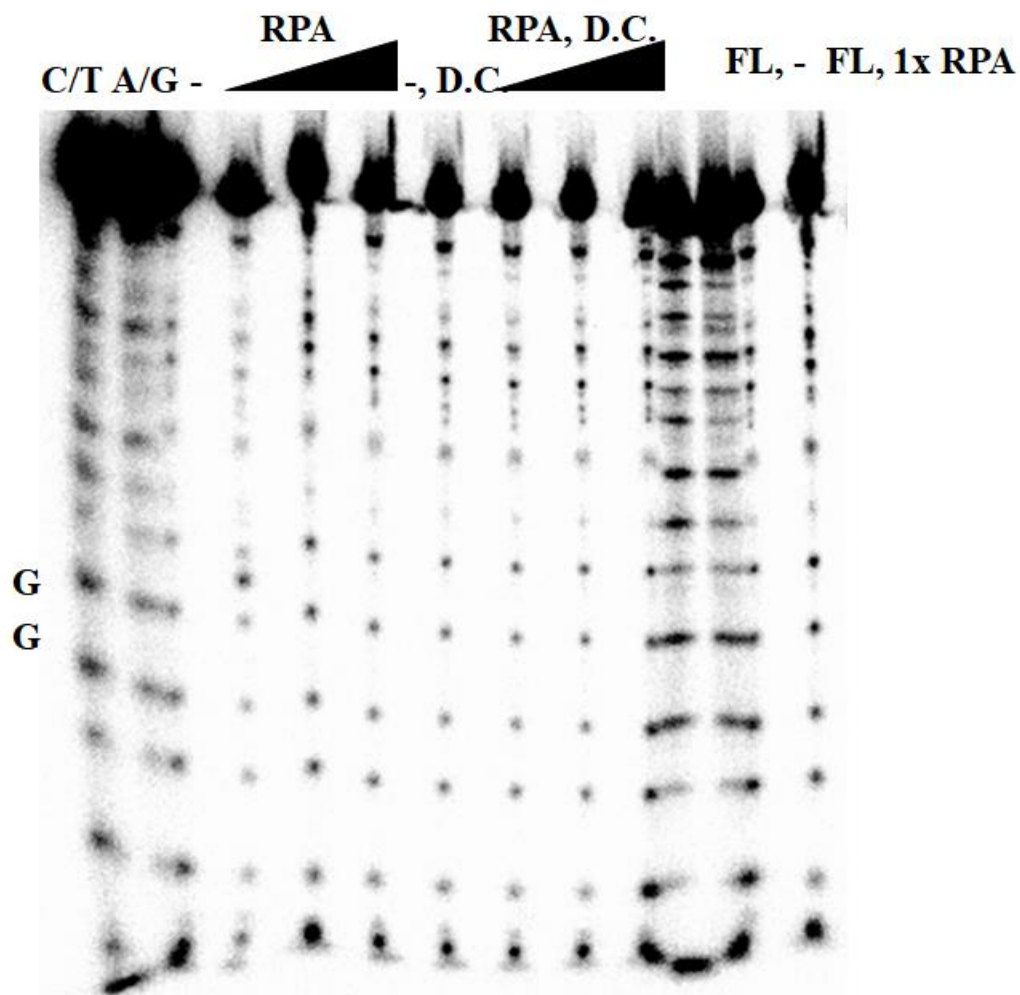


Figure 8.8 20% denaturing polyacrylamide gel containing RPA reactions alongside controls. No apparent differences are present between any reactions. Furthermore, both dark controls (D.C.) and Maxam-Gilbert sequencing lanes also show indiscriminate cleavage products. The damage seen in this gel is likely the result of overly long (several days) storage post-reaction, allow time for ^{32}P -induced damage even after piperidine removal. The DNA substrate contained a 25 nt gap, and reactions were run in the presence of 0.2 mg/mL BSA, 150 mM NaCl, and 10% glycerol v/v in 50 mM Tris-HCl, pH 7.8.

References

- 1) Burgers, P.M.; Kunkel, T.A. Eukaryotic DNA Replication Fork. *Annu. Rev. Biochem.* **2017**, *86*, 417 – 438.
- 2) Berti, M.; Vindigni, A. Replication Stress: Getting Back on Track. *Nat. Struct. Mol. Biol.* **2016**, *23*, 103 – 109.
- 3) Bartels, P.L.; Stodola, J.L.; Burgers, P.M.J.; Barton, J.K. A redox role for the [4Fe4S] cluster of yeast DNA polymerase δ . *J. Am. Chem. Soc.* **2017**, *139*, 18339 – 18448.
- 4) O'Brien, E.; Holt, M.E.; Thompson, M.K.; Salay, L.E.; Ehlinger, A.C.; Chazin, W.J.; Barton, J.K. The [4Fe4S] cluster of human DNA primase functions as a redox switch using DNA charge transport. *Science* **2017**, *355*, 6327.
- 5) McDonnell, K.J.; Chemler, J.A.; Bartels, P.L.; O'Brien, E.; Marvin, M.L.; Ortega, J.; Stern, R.H.; Raskin, L.; Li, G.; Sherman, D.H.; Barton, J.K.; Gruber, S.B. A Human MUTYH Variant Linking Colonic Polyposis to Redox Degradation of the [4Fe4S]²⁺ Cluster. **2018**, *Submitted*.
- 6) Jain, R.; Vanamee, E.S.; Dzikovski, B.G.; Buku, A.; Johnson, R.E.; Prakash, L.; Prakash, S.; Aggarwal, A.K. An iron-sulfur cluster in the polymerase domain of yeast DNA polymerase ϵ . *J. Mol. Biol.* **2014**, *426*, 301 – 308.
- 7) Netz, D.J.A.; Stith, C.M.; Stümpfig, M.; Köpf, G.; Vogel, D.; Genau, H.M.; Stodola, J.L.; Lill, R.; Burgers, P.M.J.; Pierik, A.J. Eukaryotic DNA polymerases require an iron-sulfur cluster for the formation of active complexes. *Nat. Chem. Biol.* **2012**, *8*, 125 – 132.
- 8) Pokharel, S.; Campbell, J.L. Crosstalk between the nuclease and helicase activities of Dna2: role of an essential iron-sulfur cluster domain. *Nucleic Acids Res.* **2012**, *40*, 7821 – 7830.
- 9) Alseth, I.; Eide, L.; Pirovano, M.; Rognes, T.; Seeberg, E.; Bjørås, M. The *Saccharomyces cerevisiae* homologues of Endonuclease III from *Escherichia coli*, Ntg1 and Ntg2, are both required for efficient repair of spontaneous and induced oxidative damage in yeast. *Mol. Cell. Biol.* **1999**, *19*, 3779 – 3787.
- 10) Aspinwall, R.; Rothwell, D.G.; Roldan-Arjona, T.; Anselmino, C.; Ward, C.J.; Cheadle, J.P.; Sampson, J.R.; Lindahl, T.; Harris, P.C.; Hickson, I.D. Cloning and characterization of a functional human homologue of *Escherichia coli* endonuclease III. *Proc. Natl. Acad. Sci. USA* **1997**, *94*, 109 – 114.
- 11) Arnold, A.R.; Grodick, M.A.; Barton, J.K. DNA Charge Transport: from Chemical Principles to the Cell. *Cell Chem. Biol.* **2016**, *23*, 183 – 197.

- 12) Boal, A.K.; Barton, J.K. Electrochemical Detection of Lesions in DNA. *Bioconj. Chem.* **2005**, *16*, 312 – 321.
- 13) Fanning, E.; Klimovich, V.; Nager, A.R. A dynamic model for replication protein A (RPA) function in DNA processing pathways. *Nucleic Acids Res.* **2006**, *34*, 4126 – 4237.
- 14) Bochkareva, E.; Korolev, S.; Lees-Miller, S.P.; Bochkarev, A. Structure of the RPA trimerization core and its role in the multistep DNA-binding mechanism of RPA. *The EMBO J.* **2002**, *21*, 1855 – 1863.
- 15) Wagenknecht, H.A.; Rajski, S.R.; Pascaly, M.; Stemp, E.D.; Barton, J.K. Direct observation of radical intermediates in protein-dependent DNA charge transport. *J. Am. Chem. Soc.* **2001**, *123*, 4400 – 4407.
- 16) Fan, J.; Pavletich, N.P. Structure and conformational change of a replication protein A heterotrimer bound to DNA. *Genes & Dev.* **2012**, *26*, 2337 – 2347.
- 17) Nuñez, M.E.; Noyes, K.T.; Barton, J.K. Oxidative Charge Transport through DNA in Nucleosome Core Particles. *Chem. & Biol.* **2002**, *9*, 403 – 415.
- 18) Schaefer, K.N.; Barton, J.K. DNA-Mediated Oxidation of p53. *Biochemistry* **2014**, *53*, 3467 – 3475.
- 19) Arunkumar, A.I.; Klimovich, V.; Jiang, X.; Ott, R.D.; Mizoue, L.; Fanning, E.; Chazin W.J. Insights into hRPA32 C-terminal domain-mediated assembly of the simian virus 40 replisome. *Nat. Struct. Mol. Biol.* **2005**, *12*, 332 – 339.
- 20) Homlin, R.E.; Dandliker, P.J.; Barton, J.K. Synthesis of Metallointercalator-DNA Conjugates on a Solid Support. *Bioconj. Chem.* **1999**, *10*, 1122 – 1130.
- 21) Olmon, E.D.; Hill, M.G.; Barton, J.K. Using Metal Complex Reduced States to Monitor the Oxidation of DNA. *Inorg. Chem.* **2011**, *50*, 12034 – 12044.